Dual Frequency Microwave Resonator for Non-invasive detection of Aqueous Glucose

Pejman Mohammadi[1], Ali Mohammadi[2], Member, IEEE, and Ali Kara[3], Senior Member, IEEE

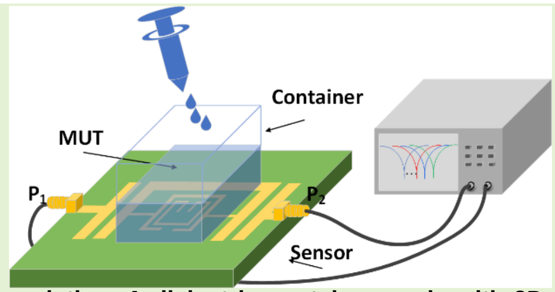

***Abstract*— A novel dual band microwave sensor for non-invasive detection of glucose concentration is presented. The proposed sensor consists of an open loop resonator coupled to the input and the output of the structure. The resonator is loaded with a modified split ring resonators for dual band operation as sensing area. The open loop resonator with electric coupling operating at low band functions as host. The SRRs embedded into the open loop resonator operates at high band. In the proposed sensor, the overall size is miniaturized using the embedded resonator structure. This configuration has two transmission poles and one transmission zero in transmission coefficients, which are all sensitive to glucose level variation. A dielectric container made with 3D printer is used for dropping the aqueous glucose samples on the sensing section of the sensor. The experimental results obtained from prototype having a dielectric container shows two resonance frequencies at 1.8 GHz and 2.67 GHz as well as a transmission zero at 2.32GHz. Glucose solution with deionized water in the range from 89 mg/dL to 456 mg/dL is used in the measurements. For this range of glucose concentrations, the experimental frequency resolutions are 0.78 MHz / (mg/dL) and 0.95 MHz / (mg/dL) based on the transmission pole and the transmission zero, respectively.**

***Index Terms*—Dual frequency, input/output coupling, glucose**

I. Introduction

THE interaction of electromagnetic wave (EM) with material has been investigated greatly for microwave sensor development toward material characterization [1-3]. With enhanced sensitivity and ease of fabrication, microwave sensors replace expensive optical, chemical and image sensing devices to measure dielectric properties of materials [1,4]. Label free characterization, and real-time responses significantly enhance microwave sensor performances. Moreover, the planar structure of microwave sensors facilitates integration with microwave planar circuits in order to make a self-sustained system in accurately measuring the dielectric constant [5]. Biomedical sensing devices operating in RF and microwave spectrum have widely been reported [6-8]. Blood glucose level (BGL) estimation is particularly investigated in [9-12]. Operation principle of these sensors is based on dielectric constant variation as a function of glucose concentration. Typical range of blood glucose in healthy people should be in the range of 70 mg/dL to 110 mg/dL in the fasting state and 70 mg/dL to 140 mg/dL post meal [7]. Diabetes Mellitus (DM) is a metabolic disease that disables the human body's natural mechanism to regulate the Blood Glucose Levels (BGL). The common method to BGL diagnoses, needs blood samples taken by skin piercing and then applied to a test strip. This type of invasive technique discomforts the patients and the process has the risk of blood-related infection [8]. On the other hand, minimally invasive implantable [9] or non-invasive sensors [10-12] allow users to test their glucose level without prick off their fingers. Hence, there are many research activities for non-invasive BGL detection. Majority of the proposed systems are based on optical techniques. The scattering of light at some chosen wavelengths is utilized to detect concentration of glucose using some optical parameters. Optical techniques have relatively lower signal-to-noise ratio. They also have inherent errors due to calibration drifts as well as thermal noise (for example body temperature), and environmental effects like humidity. Microwave sensor technology is promising for accurate and non-invasive monitoring of the BGL. Diabetes has been increasing according to International Diabetic Federation Report [13]. Although non-invasive microwave sensor seems to be effective for monitoring BGL of diabetes, however, the microwave techniques have still accuracy problems for glucose meter [14].Therefore, many efforts are put forward for non-invasive BGL measurements accurately. Transmission line techniques [15] as well as microwave resonators of various configurations [16] are used. Split ring resonator (SRR) incorporating interdigital capacitor (IDC) is used for enhanced electric field concentration leading to sensitivity in the order of 10^{-4} [17]. Three cells of complementary split ring resonators

This work was partially supported by TUBITAK (The Scientific and Technological Research Council of Turkey) and MSRT (The Ministry of Science, Research and Technology, Islamic Azad University) within Bilateral Cooperation Program (Grant #122N967, 02/13/41257).

Pejman Mohammadi is with the Microwave and Antenna Research Center, Urmia Branch, Islamic Azad University, Urmia, Iran. (e-mail: p.mohammadi@ iaurmia.ac.ir).

Ali Mohammadi is with the Department of Electronic and Electrical Engineering, University of Bath (e-mail: a.mohammadi@bath.ac.uk).

Ali Kara is with the Department of Electrical and Electronics Engineering, Faculty of Engineering, Gazi University, Ankara 06570, Turkey (e-mail: akara@gazi.edu.tr).

(CSRRs) etched on a ground plane of a dielectric resonator has been reported to achieve relatively high sensitivity [18]. However, the concentration range of blood samples are relatively small (70-120 mg/dL). A microwave BGL sensor having two resonant frequencies for increasing the accuracy and sensitivity (10^{-2}) is reported in [19]. Substrate Integrated Waveguide (SIW) with IDC are utilized as host and sensing section in [20], respectively. However, experimental results show that it has relatively low frequency detection resolution (FDR). Slow wave antenna [21] is demonstrated successfully for monitoring the aqueous glucose solution for on-body glucose measurements. Although the proposed sensor design is based on end-fire radiation, it fails to avoid perturbation of ambient electromagnetic interferences. The use of parallel resonators [22] and defected ground-structure (DGS) coplanar waveguide (CPW) array [23] are developed for glucose concentration measurements. These non-invasive techniques achieve relatively low frequency sensitivity. On the other hand, microfabrication techniques are explored to design highly sensitive microwave sensors using LC resonator [24] along with stepped-impedance resonators (SIRs) [25]. It is evident that micro-fabrication technology has a potential to miniaturize sensors. However, this technology is expensive in comparison with printed circuit board (PCB). A microfluidic microwave sensor made of microstrip transmission line loaded with a shunt-connected series LC resonator for complex permittivity detection shows large sensitivity with small volume of liquid under test (LUT) [26]. A differential microwave microfluidic sensor is robust against cross sensitivities caused by external factors [27]. A planar microwave sensor based on a composite resonator (step impedance resonator and CSRR) [28] and an extremely sensitive microfluidic sensor using transmission line loaded with shunt LC resonator [29] are reported for microfluidic characterization. However, the fabrication of microfluidic devices and alignment on sensing area are complicated processes in comparison with a container for LUT mounted on printed circuit boards (PCB). Metamaterial-inspired open-loop resonators are coupled to transmission line in order to characterize commonly available high permittivity liquids [30]. The proposed sensor shows broad permittivity range for LUT. An ultrasensitive technique is reported for non-invasive glucose sensor in which loss is compensated using active mode operation to enhance the quality factor [31]. In [32] a microwave sensor for liquid characterization with two identical CSRRs is studied. The machine learning is used to provide high resolution response.

This paper presents a novel compact size and highly sensitive microwave sensor for real-time glucose detection with aqueous solutions. The proposed sensor comprises a BPF as a host and modified SRRs as sensing area. The input/output coupling mechanism [33-34] for BPF operation is developed to respond near to industrial scientific medical (ISM) band. Modified SRRs are etched between the input and the output of the host. On the other hand, a transmission zero (TZ) is generated between two transmission poles (TPs) of the BPF. The produced TZ and TPs are used for sensory operation of the proposed configuration. The dual band operation of the proposed sensor is accomplished with a pair of SRRs. The major contributions of the paper can be summarized as follows

- Independently tuned dual band operation is demonstrated.
- SRRs is embedded into an open loop resonator so that the sensor dimension is reduced.

Based on this new configuration, the designed sensor is more immune to noise and environmental effect when compared with single-band sensors. The operation band of the proposed sensor (ISM band) is a license free band with applications in home and building automation. These applications make the proposed sensor, which is designed for usage at home/hospital environment vulnerable to interference with other technologies like Bluetooth, WiFi and devices such as microwave oven and healthcare monitoring systems [35]. Therefore, in the proposed sensor we have multiple sensitive poles/zero so that if one is affected by interference the others could be used to check the validity of measurement. This feature offers higher robustness against interferences. SRRs and CSRRs have many applications in microwave sensor and radar sensor systems [36-38].

The remaining parts of the paper is organized as follows. In section II, the topology of the dual band operation along with electromagnetic simulations are presented. Theoretical sensitivity along with the effects of sensor dimensions on TZ and transmission poles (TPs) are discussed. Section III describes glucose aqueous preparation and measurement setup as well as the analysis of the effects of dielectric container on the frequency response of the proposed sensor. Experimental sensitivity analysis based on TZ and TPs is given as well. The conclusions are drawn in section IV.

II. Proposed Design

It is known that variation in glucose concentration in aqueous solutions results in changes in the electrical characteristics of microwave biosensors [10]. Therefore, a common design principle is based on TZs or resonant frequency shifts with electrical properties of material under test (MUT). For glucose/water solutions, variation of the glucose concentration results in a variation of resonant frequency or TZ due to the change of the effective permittivity. Therefore, the proposed sensor design is based on this principle.

A. Sensor Design

The proposed sensor topology has a host and a sensing section as in most of the microwave material characterization sensors. The host of the proposed sensor is a band pass filter (BPF) that provides input-output coupling. It has smaller size compared with open loop resonators and SIRs [33]. The sensor configuration is shown in Fig. 1. Fig. 1 (a) presents the dual band input-output coupling BPF, and Fig. 1 (b) presents a modified SRRs symmetrically etched in BPF so that a TZ is generated in transmission coefficient of the structure. The design of the sensor can be detailed as follow. Firstly, a band pass filter is designed with the targeted passband characteristics (the reflection and transmission characteristics, or zeros and poles). Next, SRRs are added within the BPF and consequently, the transmission zero (TZ) appears while the transmission pole is shifted to some higher frequencies. Finally, SRR is enlarged through the upper gap, and so another transmission pole appears. The design focuses around ISM band operation of the sensor. Some of the simulations are given in the following sections.

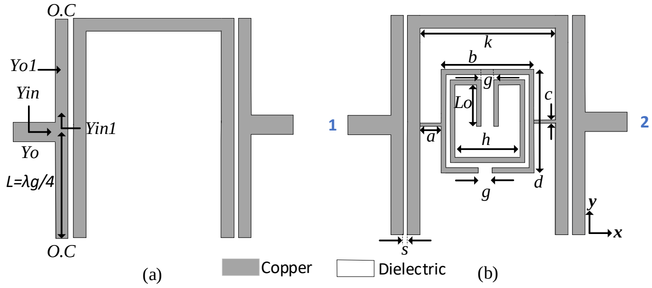

Fig. 1. Schematic of proposed (a) BPF (b) sensor

The input microstrip line with the characteristic admittance Y_0 is connected to parallel combination of two open stubs (Y_{01}). Therefore, the input admittance seen by the input microstrip line (Y_{in}), could be written, using the input admittance of each open stub, as

$$Y_{in} = 2jY_{o1}\tan(\beta l) \tag{1}$$

The impedance matching in proposed design could be achieved by choosing $Z_0 = 50\Omega$ and $Z_{in1} = 100\Omega$. Then, the width of input microstrip line and open stubs are 3.1mm and 0.7mm, respectively, for an FR4 substrate with $h = 1.6mm$, $tan\delta = 0.018$, $\varepsilon_r = 4.3$.

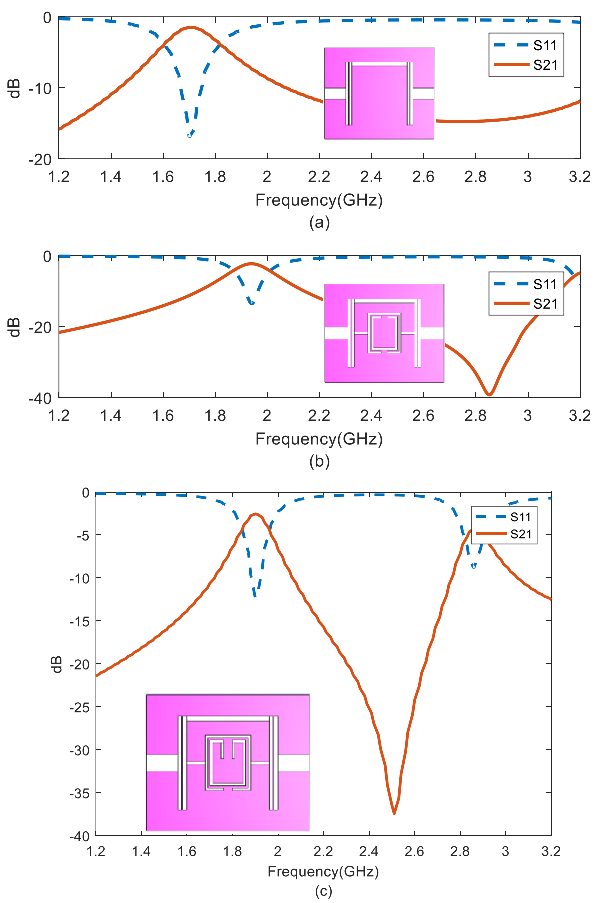

Fig. 2. Simulation results of (a) BPF (b) BPF with SRRs (c) BPF with modified SRRs.

The design procedure for the proposed sensor includes a BPF with frequency response that is shown in Fig. 2 (a) with one TP. The SRRs which are etched inside the BPF lead to a shift in TP1 and a TZ generation in transmission coefficient as shown in Fig. 2 (b). The proposed SRRs are modified with two microstrip line extensions in order to providing the desired frequency response of the proposed sensor which includes a TZ between two poles (2.516 GHz) as shown in Fig. 2 (c). Hence, a dual band operation can be achieved. The electric field distribution of the proposed sensor at the transmission frequencies (poles) is presented in Fig. 3. Fig. 3 (a) indicates that the first pole (1.9GHz) is rather dependent on the outer ring of the sensing area. On the other hand, Fig. 3 (b) shows that the second pole (2.86 GHz) is the transmission path created with the inner ring of the sensing section. The geometrical parameters of the proposed are presented in TABLE I.

TABLE I
GEOMETRICAL PARAMETERS OF THE PROPOSED SENSOR

a	b	c	d	Lo	g	h	s	k
3.41	8.4	0.5	10.2	3	1.5	5.6	0.2	15.23

Length in mm.

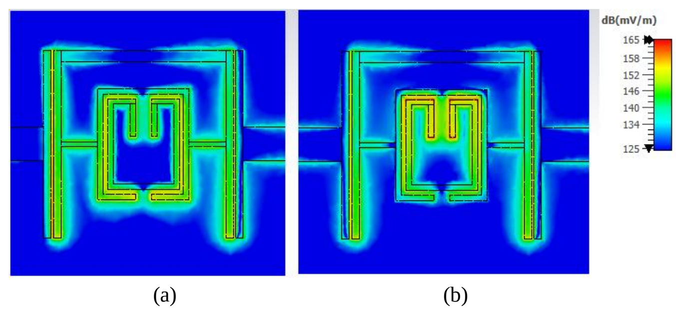

Fig. 3 Electric field distribution at (a) 1.9 GHz (b) 2.86 GHz

B. Sensor Sensitivity

Sensitivity analysis of the proposed sensor is carried out by simulations of the loaded sensor. MUTs with a variety of dielectric constants are used in the simulations. The highest permittivity ($\epsilon_r = 73$) is chosen such that it represents a typical glucose concentration of a diabetic person. Permittivity of DI-glucose solution are found using Deby coefficients [10]. Corresponding TZ and TPs for different values of permittivity is listed in TABLE II. Normalized sensitivity can be found as

$$S\% = \frac{\Delta TZ}{f_o \Delta \epsilon_r} \times 100 \tag{2}$$

where ΔTZ is the shift in the resonant frequency, $\Delta \epsilon_r$ is the permittivity variation, and f_0 is the TZ for the unloaded sensor.

TABLE II
TZ AND TPS FOR DIFFERENT PERMITTIVITY VALUES

	ϵ_r					
	24	30	41	51	62	73
TZ(GHz)	2.31	2.09	1.79	1.60	1.48	1.37
TP_1	1.04	0.96	0.83	0.76	0.70	0.65
TP_2	1.89	1.77	1.59	1.47	1.37	1.30

The normalized theoretical sensitivity of the proposed sensor is found to be 0.76 when a MUT of thickness 2mm is taken. The normalized sensitivity can also be calculated as 0.42 based on the TPs with TP_{10}= 1.9 GHz and TP_{20}= 2.86 GHz, in (2) for the unloaded sensor. In order to investigate the sensitivity of TZ and TPs, simulation results for MUTs with different dielectric constants are provided in Fig. 4. For MUTs with relatively lower dielectric constants, the sensitivity of TZ is higher in comparison with the sensitivity of TPs. The frequency shift and normalized sensitivity, based on (2), are listed in Table III. This demonstrates superiority of using TZ instead of TPs.

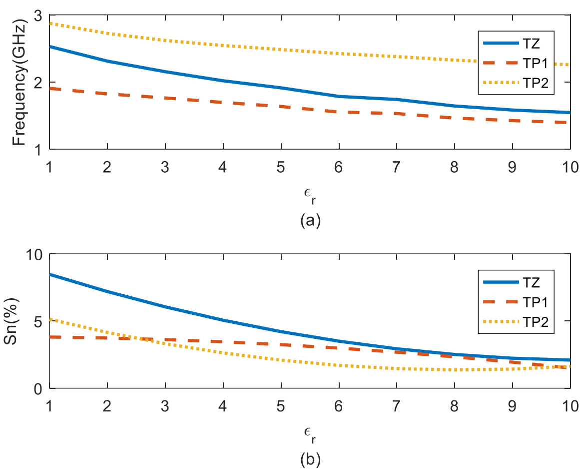

Fig. 4 (a) TZ and TPs variation (b) normalized sensitivity for change in MUT permittivity.

TABLE III
THEORETICAL SENSITIVITY OF TZ AND TPS

	$\Delta f(GHz)$	$f_0(GHz)$	$S\%$
TZ	0.9825	2.5	4.2
$TP1$	0.51	1.9	2.97
$TP2$	0.615	2.8	2.37

The TZ values of most of microwave sensors are dependent on the MUT thickness. This is due to the fact that microwave sensors operate on near field as explained by lift-off analysis [39]. We investigate this mechanism with conducting simulations with different MUT thicknesses and constant permittivity ($\epsilon_r = 73$) for the proposed sensor.

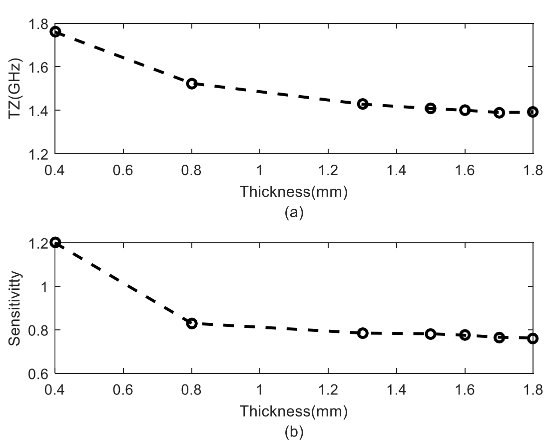

Fig. 5 The effect of MUT thickness on (a) TZ (b) theoretical sensitivity

The variation of TZ with respect to the thickness is shown in Fig. 5 (a). It seems that, firstly, the TZ decreases smoothly with increasing thickness. It converges to 1.4 GHz at around the thickness of 1.6 mm for the proposed sensor. Next, the sensitivity of the proposed sensor with respect to thickness is plotted in Fig. 5 (b), based on (2). It should be noted the sensitivity is highly dependent on thickness within the range of 0.4mm-1.6mm, and then it is almost constant for the thickness above this range.

C. Sensor Size Effects on TZ

The variation of the TZ with respect to permittivity change is major concern for sensitivity assessment in such sensor configurations. On the other hand, the range of TZ is of interest to biomedical applications point of view. The range of TZ of the proposed sensor configuration is calculated through the SRRs loading of the host. Therefore, we investigated the effects of the SRRs dimensions on the TZ values as in Fig. 6. Shown in Fig. 6 (a) is the variation TZ with respect to the length of SRRs (Lo). Increasing the length of SRRs results in longer current path from which the inductive effect increases and then the TZs are reduced. Moreover, the higher TP is changing with SRRs length variation while the lower TP is almost constant as expected from electric field distribution in Fig. 3. It is found that higher TP could adjusted independently from lower TP with (Lo) tuning. The two gaps in Fig. 1 (b) could also influence the TZ value. Fig. 6 (b) reveals that the higher the gap (g) leads to the lower TZ value. This could be attributed to the capacitive effect in the open end of SRRs. Increasing the gap (g) leads to lower capacitive effect and consequently TZ is increased. In addition, higher TP shows more decrement compared with lower one. As the targeted TZ is 2.516 GHz for the proposed sensor, the length (Lo) and the gap (g) are selected to be 3 mm and 1.5 mm, respectively.

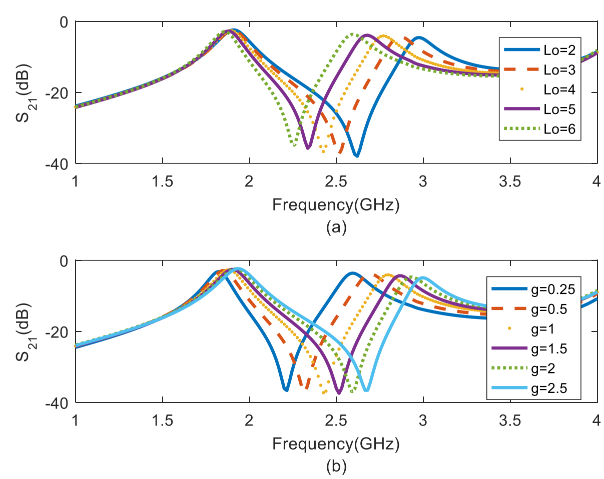

Fig. 6 TZs variation with respect to SRRs (a) Length (b) gap

III. EXPERIMENTS

A prototype sensor is fabricated in order to validate the proposed design. Some aqueous solutions (AQs) are prepared from glucose powder in deionized water. Then, the aqueous solutions are examined for glucose level detection with a standardized medical instrument ("biotecnica instruments" model BT1500). The measurement results from the medical instrument are summarized in Table IV. The measurement setup is shown in Fig. 7 (a). As can be seen, dielectric container is fixed on the top of the prototype sensor for dropping the liquid in the sensing section. The size of container at the thin base section is 1 mm×1.2 mm×0.16 mm, and it is placed symmetrically on the sensing area. Two plastic clips are used to fix the container on the sensor, as shown in Fig. 7 (b). The 200 µL of prepared AQs are poured into the container with a pipette. This amount is determined based on the container dimensions in Fig. 5. It is intended to neutralize the effect of the MUT thickness on the TZ as well as the sensitivity. The simulated and measured S-parameters of the proposed sensor is shown in Fig. 7 (c). It should be noted that there is a frequency shift between the two responses. This discrepancy could be originated from fabrication error, dielectric constant variation and/or measurement error. Testing of the AQ is repeated five times, and then container is cleaned to dry completely in order to minimize the measurements error. In each measurement trial, TPs and TZs are recorded. The mean values of the TPs and the TZs for a bare sensor with the container as well as with different GL AQs within container is summarized in Table V.

TABLE IV
GL(mg/dL) OF PREPARED FROM MEDICAL INSTRUMENT

G_L Prepared	G_L Hospital	Relative Error (%)
100	89	11
130	119	8.5
350	333	4.8
450	456	1.3

TABLE V
MEASURED TZS AND TPS

G_L (mg/dL)	TZ(GHz)	TP$_2$ - TP$_1$ (GHz)
Bare	2.32	2.67- 1.79
89	1.86	2.36- 1.55
119	1.90	2.39 – 1.58
333	2.11	2.56 – 1.69
456	2.21	2.64 – 1.72

The dielectric container placed on the sensing area leads to a slight frequency shift of the transmission characteristic, as shown in Fig. 8, which is considered in experimental sensitivity estimation. The variation of the TZ and TPs are illustrated in Fig. 8 (a) and Fig. 8 (b), respectively. Moreover, the transmission and reflection coefficients of the proposed sensor with empty container and then loaded with MUT samples are shown in Fig. 9. It should be noted that that the TZs and the TPs of the proposed sensor are shifted. Another performance parameter of glucose concentration detection sensors is the frequency detection resolution (FDR). The FDR in $MHz/(mg/dL)$ can be extracted as [19]

$$FDR = \frac{\Delta F}{\Delta C} \tag{3}$$

where ΔF is the frequency shift of TZ or TPs, and ΔC is the variation of the glucose. For the testing of the proposed sensor, GL is increased from 89 mg/dL to 456 mg/dL, resulting in a ΔC of 367 mg/dL. The corresponding TZ and TPs variations are found to be $\Delta F_{TZ} = 350\ MHz$, $\Delta F_{TP2} = 280\ MHz$ and

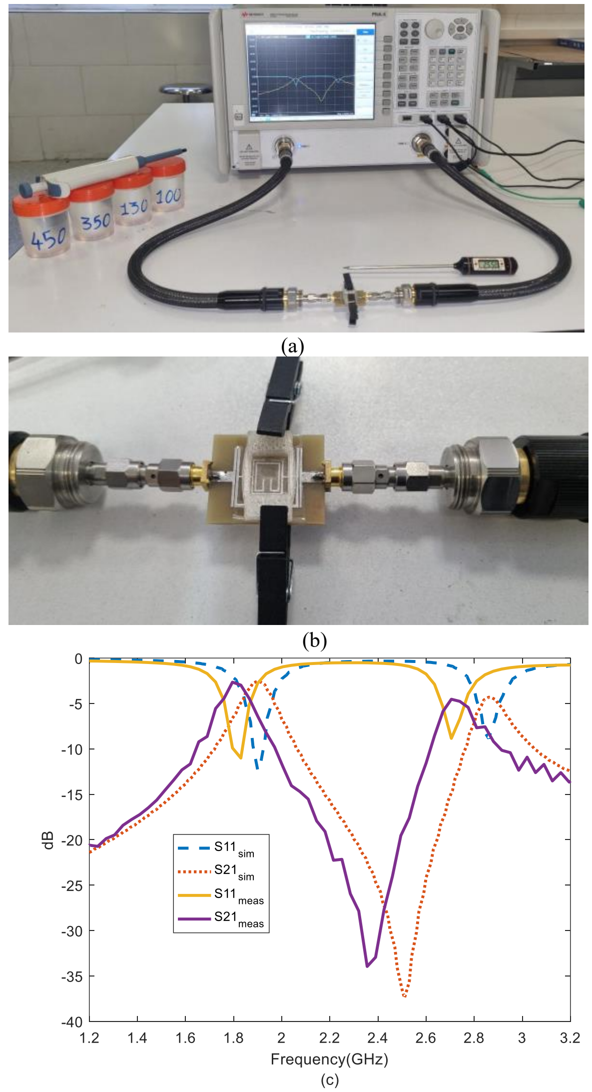

Fig. 7 (a) Measurement setup (b) the sensor with dielectric container (c) Measured and simulated S parameters.

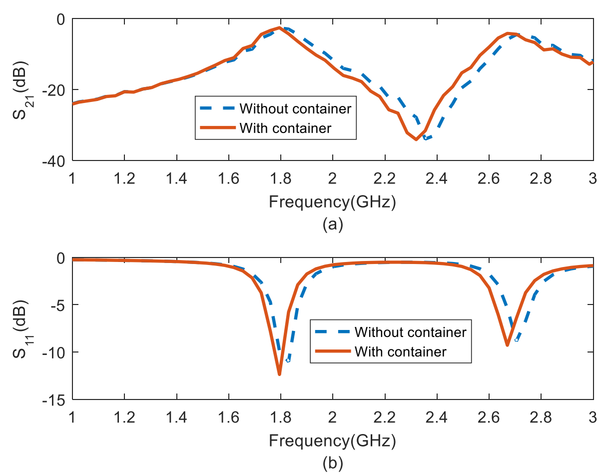

Fig. 8 Transmission (a) and reflection (b) coefficients of the proposed sensor with and without container

$\Delta F_{TP1} = 175\ MHz$, respectively. Therefore, the FDR of the TZ is higher than that of the TPs. Different BGL sensors might have different FDR values as the resonant frequency of the sensors might be different. Hence, the following normalized sensitivity in $1/(mg/dL)$ is adopted in order to compare the sensors fairly [19]

$$S_n = \frac{\Delta F}{f_0 \Delta C} \times 100 \quad (4)$$

where f_0 is the TZ of the bare sensor. For the proposed sensor, f_0 is 2.32 GHz, which is measured from the sensor with dielectric container on top of it, and S_n is 0.041.

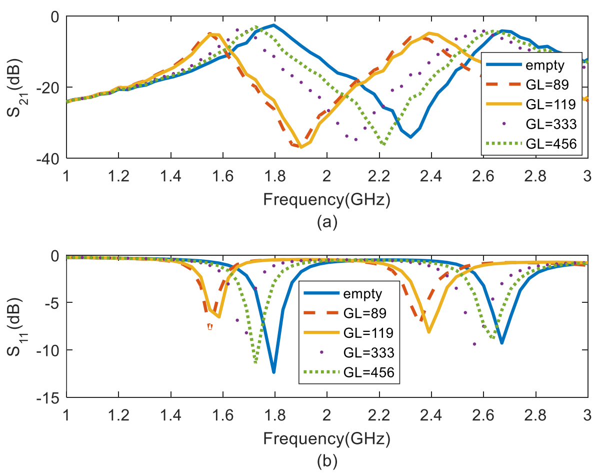

Fig. 9 Transmission (a) and reflection (b) coefficients of the proposed sensor for AQ with different GL values.

The variation of the measured sensitivity with respect to GL is widely reported in glucose detection sensors [10, 22]. For the proposed sensor, the following polynomial curve fitting technique is utilized based on the experimental data of Table V.

$$f = ax^3 + bx^2 + cx + d \quad (5)$$

The polynomial coefficients for the TZ and the TPs are summarized in Table VI. Next, the following experimental normalized sensitivity is obtained.

$$S_n = \frac{\partial f}{f_0 \partial x} \times 100 \quad (6)$$

where f is TZ or TPs and x is GL.

TABLE VI
POLYNOMIAL COEFFICIENTS FOR TZS AND TPS

Coefficients	TZ(GHz)	TP_2 (GHz)	TP_1 (GHz)
a	2.57E-09	1.886E-09	3.243E-09
b	-2.833E-06	-2.45E-06	-3.746E-06
c	0.001839	0.001615	0.001673
d	1.717	2.229	1.428

Fig. 10 (a) presents the variation of the TZ and the TPs with respect to the measured GL. The maximum value for uncertainty is around ±12 MHz. The normalized sensitivity variations, based on the TZ and the TPs, with respect to GL are shown in Fig. 10 (b). The normalized sensitivity based on the TZ is higher than that of the TPs. Note that, lower the GL is higher the sensitivity. The sensitivity tends to increase after the GL of 400 mg/dL.

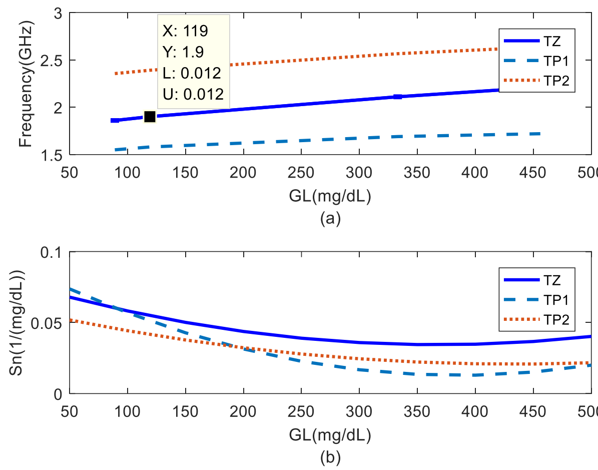

Fig. 10 The variation of (a) TZ, TP1 and TP2 (b) the normalized measured sensitivity with the GL

The electrical performances of the proposed sensor are compared in Table VII, with similar sensors reported in literature. It should be noted that the sensors reported in [24,25] and the proposed sensor outperforms all other sensors. Also note that a costly manufacturing technique, compared to PCB, (microfabrication) is used in [25].

The sensors reported in [31-32] show lower sensitivity compared with the propose sensor. Note that it is a convention that the size of the sensing section is normalized to the guided wavelength (λ_g) for comparison of the sensors. As can be seen, the size of the proposed sensor is smaller than that of similar sensors except the one reported in [22]. An external readout circuit is employed for connection with MUT in [22], and the sensor size is not reported.

TABLE VII
COMPARISON OF PROPOSED SENSOR WITH AVAILABLE BGL SENSORS

Ref.	Concentration (mg/dL)	$f_0(GHz)$	$S(\frac{MHz}{mg/dL})$	$S_n\left(\frac{1}{mg/dL}\right)$	MUT	Size (λ_g^2)
[17]	0-5000	4.18	0,026	6.2E-4	A.G	0.016
[18]	70-120	50-70	1.2	2E-3	A.G	10.17
[19]	89-262	8.5, 5.5	3.58, 3.53	4E-2, 6E-2	Finger	0.5
[21]	75-150	8.8	1.5	1.7E-2	A.G	1.5
[22]	0-500	1.016, 2.87	0.046,0.5	4E-3, 1.7E-2	A.G	0.001
[23]	0-1800	4.4725	0.0039	8.7E-5	A.G	0.02
[24]	30-500	1.5	1.175	7.45E-2	A.G	-
[25]	75-500	6.53	40.58	6.2E-2	A.G	-
[31]	18-540	1.156	7.5E-5	6.48E-6	A.G	0.02
[32]	-	3.5	-	3E-2	A.G	-
Proposed	89-456	2.32	0.95	4.1E-2	A.G	0.017

A.G=Aqueous Glucose

In order to have fair comparison with existing microwave sensors, the measurement data are used in conjunction with Deby relaxation [10] to obtain complex permittivity. The TZ, TPs and sensitivity variations with respect to dielectric constant are shown in Fig. 11 (a) and Fig. 11 (b), respectively. Increasing the dielectric constant reduces TZs whereas this increase the sensitivity.

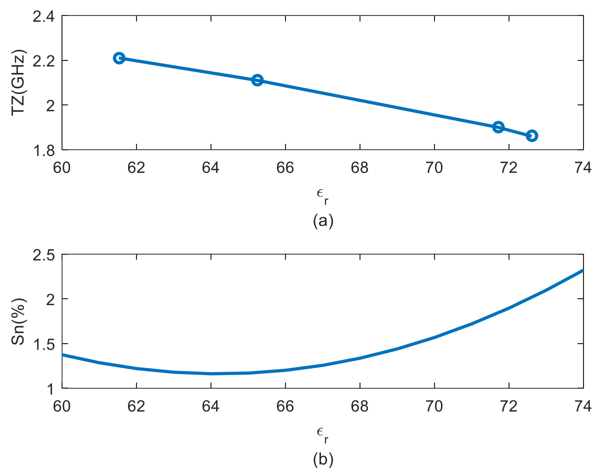

Fig. 11 (a) Variation of the TZs with respect to dielectric constant (b) variation of the normalized sensitivity with respect to dielectric constant

This comparison shows that the sensitivity of the proposed sensor is higher than that of the sensor reported in [26] and [27]. In addition, the sensor reported in [28] measures the voltage amplitude at the operating frequency, and the sensor sensitivity is reported in mV/% and dB/%. However, variation of the transmission coefficient shows smaller sensitivity in comparison with the proposed sensor. Another design reported in [29] shows higher average sensitivity (S_{av}=1.36) compared with the proposed sensor. It should be, however, noted that the measurement is more complex as it includes outlet and inlet tubes, syringe, microfluidic channel and a plexiglass frame. Finally, the sensor reported in [30] presents a decaying sensitivity with increasing permittivity, which is lower than the sensor proposed in this work.

IV. Conclusion and Future Research

Design of compact size and highly sensitive microwave sensor for use in real-time measurement of variation of glucose level (GL) is presented in this paper. The proposed sensor configuration employs a dual mode band pass filter (BPF) along with modified splint ring resonators (SRRs). Coupling mechanism of the BPF generates the response at the targeted operational band (ISM) while the modified SRRs etched in between the input and output serves as the sensing section. The design stages of the sensor are presented in detail, and sensitivity analysis is conducted. The experimental results with the prototype show that the sensitivity of the proposed sensor is higher than that of most sensors reported in the literature. It should also be noted that the proposed sensor configuration has a potential for eliminating the environmental effects. For a future work, dual band operation of the sensor might be studied. In this way, one of the TPs, or the TZ, is kept constant with GL variation while others are perturbed by the GL variation. Therefore, the difference between the two frequencies could be used as a sensor index. Moreover, the environmental effects on both frequencies could be better removed.

References

[1] M. Abdolrazzaghi, V. Nayyeri, and F. Martin, “Techniques to Improve the Performance of Planar Microwave Sensors: A Review and Recent Developments,” Sensors, vol. 22, no. 18, p. 6946, Sep. 2022.
[2] M. G. Mayani, F. J. Herraiz-Martínez, J. M. Domingo and R. Giannetti, "Resonator-Based Microwave Metamaterial Sensors for Instrumentation: Survey, Classification, and Performance Comparison," in IEEE Transactions on Instrumentation and Measurement, vol. 70, pp. 1-14, 2021, Art no. 9503414.
[3] P. Mohammadi, A. Mohammadi and A. Kara, "T-Junction Loaded With Interdigital Capacitor for Differential Measurement of Permittivity," in IEEE Transactions on Instrumentation and Measurement, vol. 71, pp. 1-8, 2022, Art no. 8005708.
[4] P. Mohammadi, H. Teimouri, A. Mohammadi, S. Demir and A. Kara, "Dual Band, Miniaturized Permittivity Measurement Sensor With Negative-Order SIW Resonator," in IEEE Sensors Journal, vol. 21, no. 20, pp. 22695-22702, 15 Oct.15, 2021.
[5] V. Sekar, W. J. Torke, S. Palermo and K. Entesari, "A Self-Sustained Microwave System for Dielectric-Constant Measurement of Lossy Organic Liquids," in IEEE Transactions on Microwave Theory and Techniques, vol. 60, no. 5, pp. 1444-1455, May 2012.
[6] P. Mehrotra, B. Chatterjee, and S. Sen, “EM-Wave Biosensors: A Review of RF, Microwave, mm-Wave and Optical Sensing,” Sensors, vol. 19, no. 5, p. 1013, Feb. 2019.
[7] American Diabetes Association, “7. Diabetes technology: Standards of medical care in diabetes-2020,” Diabetes Care, vol. 43, no. 1, pp. S77–S88, 2020.
[8] S. K. Yee et al., “Microstrip defected ground structure for determination of blood glucose concentration,” Prog. Electromag. Res., vol. 99, pp. 35–48, Jan. 2020.
[9] R. S. Hassan, J. Lee and S. Kim, "A Minimally Invasive Implantable Sensor for Continuous Wireless Glucose Monitoring Based on a Passive Resonator," in IEEE Antennas and Wireless Propagation Letters, vol. 19, no. 1, pp. 124-128, Jan. 2020.
[10] P. Mohammadi, A. Mohammadi, S. Demir, and A. Kara, “Compact size, and highly sensitive, microwave sensor for non-invasive measurement of blood glucose level,” *IEEE Sensors J.*, vol. 21, no. 14, pp. 16033–16042, Jul. 2021.
[11] S. Y. Huang *et al.*, “Microstrip line-based glucose sensor for noninvasive continuous monitoring using the main field for sensing and multivariable crosschecking,” *IEEE Sensors J.*, vol. 19, no. 2, pp. 535–547, Jan. 2019.
[12] M. Bteich et al., "A Non-Invasive Flexible Glucose Monitoring Sensor Using a Broadband Reject Filter," in IEEE Journal of Electromagnetics, RF and Microwaves in Medicine and Biology, vol. 5, no. 2, pp. 139-147, June 2021.
[13] International Diabetes Federation, IDF Diabetes Atlas. [Online]. Available: http://www.diabetesatlas.org.
[14] M. C. Cebedio, L. A. Rabioglio, I. E. Gelosi, R. A. Ribas, A. J. Uriz and J. C. Moreira, "Analysis and Design of a Microwave Coplanar Sensor for Non-Invasive Blood Glucose Measurements," in IEEE Sensors Journal, vol. 20, no. 18, pp. 10572-10581, 15 Sept.15, 2020.
[15] M. Hofmann, G. Fischer, R. Weigel, and D. Kissinger, “Microwavebased noninvasive concentration measurements for biomedical applications,” IEEE Trans. Microw. Theory Techn., vol. 61, no. 5, pp. 2195–2204, May 2013.
[16] T. Yilmaz, R. Foster and Y. Hao, "Broadband Tissue Mimicking Phantoms and a Patch Resonator for Evaluating Noninvasive Monitoring of Blood Glucose Levels," in IEEE Transactions on Antennas and Propagation, vol. 62, no. 6, pp. 3064-3075, June 2014.
[17] G. Govind and M. J. Akhtar, "Metamaterial-Inspired Microwave Microfluidic Sensor for Glucose Monitoring in Aqueous Solutions," in IEEE Sensors Journal, vol. 19, no. 24, pp. 11900-11907, 15 Dec.15, 2019.
[18] A. E. Omer, S. Gigoyan, G. Shaker and S. Safavi-Naeini, "WGM-Based Sensing of Characterized Glucose- Aqueous Solutions at mm-Waves," in IEEE Access, vol. 8, pp. 38809-38825, 2020.
[19] S. Kiani, P. Rezaei and M. Fakhr, "Dual-Frequency Microwave Resonant Sensor to Detect Noninvasive Glucose-Level Changes Through the Fingertip," in IEEE Transactions on Instrumentation and Measurement, vol. 70, pp. 1-8, 2021, Art no. 6004608.
[20] S. Kiani, P. Rezaei, M. Karami, and R. A. Sadeghzadeh, “Band-stop filter sensor based on SIW cavity for the non-invasive measuring of blood glucose,” *IET Wireless Sensor Syst.*, vol. 9, no. 1, pp. 1–5, Feb. 2019.

[21] A. Kandwal et al., "Surface Plasmonic Feature Microwave Sensor With Highly Confined Fields for Aqueous-Glucose and Blood-Glucose Measurements," in IEEE Transactions on Instrumentation and Measurement, vol. 70, pp. 1-9, 2021, Art no. 8000309.

[22] R. S. Hassan, "Wireless and Battery-Free Biosensor Based on Parallel Resonators for Monitoring a Wide Range of Biosignals," in IEEE Transactions on Microwave Theory and Techniques, vol. 70, no. 10, pp. 4566-4578, Oct. 2022.

[23] Z. Yi and C. Wang, "Noninvasive Glucose Sensors Using Defective-Ground-Structure Coplanar Waveguide," in IEEE Sensors Journal, vol. 23, no. 1, pp. 195-201, 1 Jan.1, 2023.

[24] A. Kumar et al., "High-Sensitivity, Quantified, Linear and Mediator-Free Resonator-Based Microwave Biosensor for Glucose Detection," Sensors, vol. 20, no. 14, p. 4024, Jul. 2020.

[25] K. K. Adhikari and N. -Y. Kim, "Ultrahigh-Sensitivity Mediator-Free Biosensor Based on a Microfabricated Microwave Resonator for the Detection of Micromolar Glucose Concentrations," in IEEE Transactions on Microwave Theory and Techniques, vol. 64, no. 1, pp. 319-327, Jan. 2016.

[26] A. Ebrahimi, J. Scott and K. Ghorbani, "Ultrahigh-Sensitivity Microwave Sensor for Microfluidic Complex Permittivity Measurement," in IEEE Transactions on Microwave Theory and Techniques, vol. 67, no. 10, pp. 4269-4277, Oct. 2019.

[27] P. Vélez, L. Su, K. Grenier, J. Mata-Contreras, D. Dubuc and F. Martín, "Microwave Microfluidic Sensor Based on a Microstrip Splitter/Combiner Configuration and Split Ring Resonators (SRRs) for Dielectric Characterization of Liquids," in IEEE Sensors Journal, vol. 17, no. 20, pp. 6589-6598, 15 Oct.15, 2017.

[28] P. Vélez et al., "Single-Frequency Amplitude-Modulation Sensor for Dielectric Characterization of Solids and Microfluidics," in IEEE Sensors Journal, vol. 21, no. 10, pp. 12189-12201, 15 May15, 2021.

[29] H. Abdelwahab, A. Ebrahimi, F. J. Tovar-Lopez, G. Beziuk, and K. Ghorbani, "Extremely Sensitive Microwave Microfluidic Dielectric Sensor Using a Transmission Line Loaded with Shunt LC Resonators," Sensors, vol. 21, no. 20, p. 6811, Oct. 2021.

[30] M. Abdolrazzaghi, M. Daneshmand and A. K. Iyer, "Strongly Enhanced Sensitivity in Planar Microwave Sensors Based on Metamaterial Coupling," in IEEE Transactions on Microwave Theory and Techniques, vol. 66, no. 4, pp. 1843-1855, April 2018.

[31] M. Abdolrazzaghi, N. Katchinskiy, A. Y. Elezzabi, P. E. Light and M. Daneshmand, "Noninvasive Glucose Sensing in Aqueous Solutions Using an Active Split-Ring Resonator," in IEEE Sensors Journal, vol. 21, no. 17, pp. 18742-18755, 1 Sept.1, 2021.

[32] N. Kazemi and P. Musilek, "Enhancing Microwave Sensor Performance With Ultrahigh Q Features Using CycleGAN," in IEEE Transactions on Microwave Theory and Techniques, vol. 70, no. 12, pp. 5369-5382, Dec. 2022, doi: 10.1109/TMTT.2022.3218015.

[33] A. Gorur and C. Karpuz, "Miniature Dual-Mode Microstrip Filters," in IEEE Microwave and Wireless Components Letters, vol. 17, no. 1, pp. 37-39.

[34] L. Athukorala and D. Budimir, "Compact Dual-Mode Open Loop Microstrip Resonators and Filters," in IEEE Microwave and Wireless Components Letters, vol. 19, no. 11, pp. 698-700, Nov. 2009.

[35] W. Guo, W. M. Healy and M. Zhou, "Impacts of 2.4-GHz ISM Band Interference on IEEE 802.15.4 Wireless Sensor Network Reliability in Buildings," in IEEE Transactions on Instrumentation and Measurement, vol. 61, no. 9, pp. 2533-2544, Sept. 2012.

[36] M. S. K T, M. A. H. Ansari, A. K. Jha and M. J. Akhtar, "Design of SRR-Based Microwave Sensor for Characterization of Magnetodielectric Substrates," in IEEE Microwave and Wireless Components Letters, vol. 27, no. 5, pp. 524-526, May 2017.

[37] S. Wang, K. Li, F., Kong, L. Du, "A miniaturized triple-band planar antenna combing single-cell metamaterial structure and defected ground plane for WLAN/WiMAX applications, " in J. Electromagn. Waves Appl., vol. 35, no.3, pp. 357-370, 2021.

[38] W. Wang et al., "Wideband Gain Enhancement of MIMO Antenna and Its Application in FMCW Radar Sensor Integrated With CMOS-Based Transceiver Chip for Human Respiratory Monitoring," in IEEE Transactions on Antennas and Propagation, vol. 71, no. 1, pp. 318-329, Jan. 2023.

[39] A. Rasoulzadeh and P. Mohammadi, "Thickness Measurement of Thin Layers with Double E-Shaped Slots Loaded in a Microstrip Line," in IEEE Sensors Journal, vol. 23, no. 2, pp. 1132-1138, 15 Jan.15, 2023.

Pejman Mohammadi, received Ph.D. degree in Electrical Engineering from the Middle East Technical University Turkey. Since 2001, he has been with the Department of Electrical Engine ring, Islamic Azad University of Urmia, Iran where he is currently Associate Professor. He is also member of Microwave and Antenna Research Center, Urmia Branch, Islamic Azad University, Urmia, Iran. His research interests include microwave component SIW, microwave sensors, microstrip antennas, small antennas for wireless communications, and reconfigurable structures.

Ali Mohammadi, received PhD degree in Electrical Engineering from the University of Newcastle Australia (2014). He conducted post-doctoral research at Monash University and University of Oxford. He is Associate Professor at the Department of Electronics and Electrical Engineering, University of Bath, UK. His research interests include microelectromechanical (MEM) devices and microelectronic circuits with applications in micro-energy harvesting and high precision sensing. Dr Mohammadi received MEMS Design Awards form Europractice completions in 2018 and 2020.

Ali Kara received Ph.D. degree from Hacettepe University in 2002. He was with Polytechnic University (ECE), Brooklyn, from 1999 to 2000, where he conducted theoretical and experimental research. He joined the Department of Electrical and Electronics Engineering of Atilim University, in 2000 and worked until 2021, where he held various positions from lecturer level to full professor levels. As of April 2021, he joined the Department of Electrical and Electronics Engineering, Faculty of Engineering, Gazi University in Ankara. He has published extensively in Electromagnetics, Antennas and Propagation as well as Engineering Education. He has five patents. He had led, and has been leading some national and international projects.